Amphipolar, Amphiphilic 2,4-diarylpyrano[2,3-*b*]indoles as Turn-ON Luminophores in Acidic and Basic Media

Tobias Wilcke [1], Alexandru Postole [1], Marcel Krüsmann [2], Matthias Karg [2] and Thomas J. J. Müller [1,*]

[1]   Institut für Organische Chemie und Makromolekulare Chemie, Heinrich-Heine-Universität Düsseldorf, Universitätsstrasse 1, D-40225 Düsseldorf, Germany; t.wilcke@hhu.de (T.W.); alexandru.postole@su.se (A.P.)
[2]   Institut für Physikalische Chemie, Heinrich-Heine-Universität Düsseldorf, Universitätsstrasse 1, D-40225 Düsseldorf, Germany; marcel.kruesmann@hhu.de (M.K.); karg@hhu.de (M.K.)
*   Correspondence: thomasjj.mueller@uni-duesseldorf.de; Tel.: +49-(0)211-81-12298

Abstract: A versatile amphiphilic pyrano[2,3-*b*]indole for halochromic turn-ON luminescence in acidic or basic media is accessed by an insertion-coupling-cycloisomerization and adjusting solubilizing and phenolic functionalities. While almost non-emissive in neutral solutions, treatment with acids or bases like trifluoroacetic acid (TFA) or 1,8-diazabicyclo[5.4.0]undec-7-ene (DBU) reveals distinct luminescence at wavelengths of 540 nm or 630 nm in propan-2-ol, respectively. Turn-ON emission can be detected at pH values as mild as pH = 5.31 or 8.70. Quantum yields in propan-2-ol are substantial for protonated ($\Phi_f = 0.058$) and deprotonated ($\Phi_f = 0.059$) species. Photometrically, pK_{a1} of 3.5 and pK_{a2} of 10.5 were determined in propan-2-ol. With lipophilic polyether sidechains and hydrophilic protonation and deprotonation sites the molecule can be regarded as amphipolar, which results in good solubility properties for different organic solvents. In aqueous media, an organic co-solvent like propan-2-ol (35%) or tetrahydrofuran (25%) is needed, and the solution can be diluted with pure water without precipitation of the compound. At higher concentrations of water, a turbid solution is formed, which indicates the formation of micellar structures or clusters. With dynamic light scattering we could show that these clusters increase in size with increasing water content.

Keywords: dynamic light scattering; halochromicity; heterocycles; luminescence; sensors; UV/Vis spectroscopy

1. Introduction

Functional organic materials [1] have become increasingly important in many different fields of application, such as electronics [1–13], biomedicine [14–19], and analytics [20–28]. A rational design allows for the tailoring of the molecular property and applicability of these molecular materials [29–38]. In particular, structure-property relationships help with the understanding of the materials' characteristics, thus improving their performance. Especially in the field of analytics, stimuli responsive molecules are of great interest due to their ability to selectively and reversibly bind an analyte, while exhibiting significant and detectable changes of their molecular electronic properties, e.g., color, luminescence, or redox potentials [39–49]. Analytes that can be detected by chemosensors are manifold, ranging from biologically relevant anions and cations to protons, gases and even small neutral molecules [50–53]. Functional organic materials with sensing properties include polymers, nanoparticles, as well as small heterocyclic molecules [28,54–59]. Heterocycles with stimuli responsive changes of their photophysical properties possess significant advantages over other read-out signals. Turn-ON luminescence, for instance, can be measured against a dark background and therefore offers a high sensitivity towards analytes. Moreover, fast read-outs, low costs, and comparably simple instrumentation are further advantages of these types of turn-ON luminescence chemosensors. Other possible photophysical read-outs include chromicity responses, i.e., changes in absorption or emission bands, as well as varying signal intensities or lifetime domains [60].

Recently, we have demonstrated that 2,4-diarylpyrano[2,3-*b*]indoles are readily accessible from alkynoyl *ortho*-iodo anilides and terminal arylalkynes through a Pd-Cu-catalyzed domino insertion-coupling-cycloisomerization reaction [61,62]. Investigations of their photophysical properties revealed that halochromic luminescence in solution is induced through protonation in acid media or complexation with quantum yields of up to 15% (Scheme 1). Based on these observations, the use of 2,4-diarylpyrano[2,3-*b*]indoles as turn-ON luminophores and proton-sensitive chemosensors was considered, even expanding the solvent systems and the solubility [62].
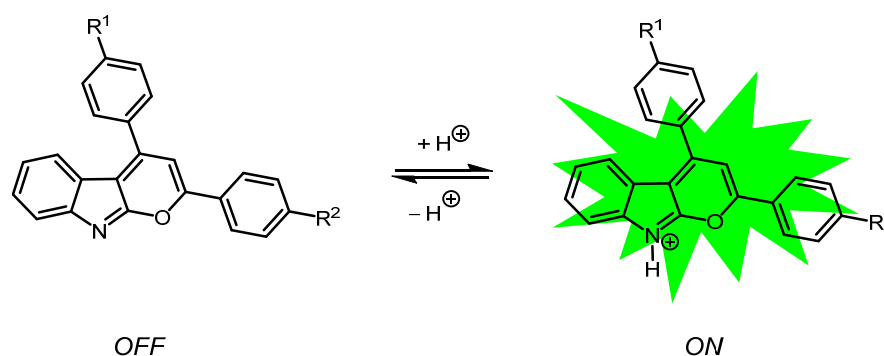

Scheme 1. Reversibly switchable halochromic turn-ON luminescent 2,4-diarylpyrano[2,3-*b*]indoles.

Herein, we disclose a novel type of versatile amphiprotic 2,4-diarylpyrano[2,3-*b*]indole system suitable for the detection of both acids as well as bases through turn-ON luminescence in organic and aqueous solutions. Besides the synthesis, photophysical characterization and particle size analysis of an amphiprotic 2,4-diarylpyrano[2,3-*b*]indole are presented and discussed.

2. Results and Discussion

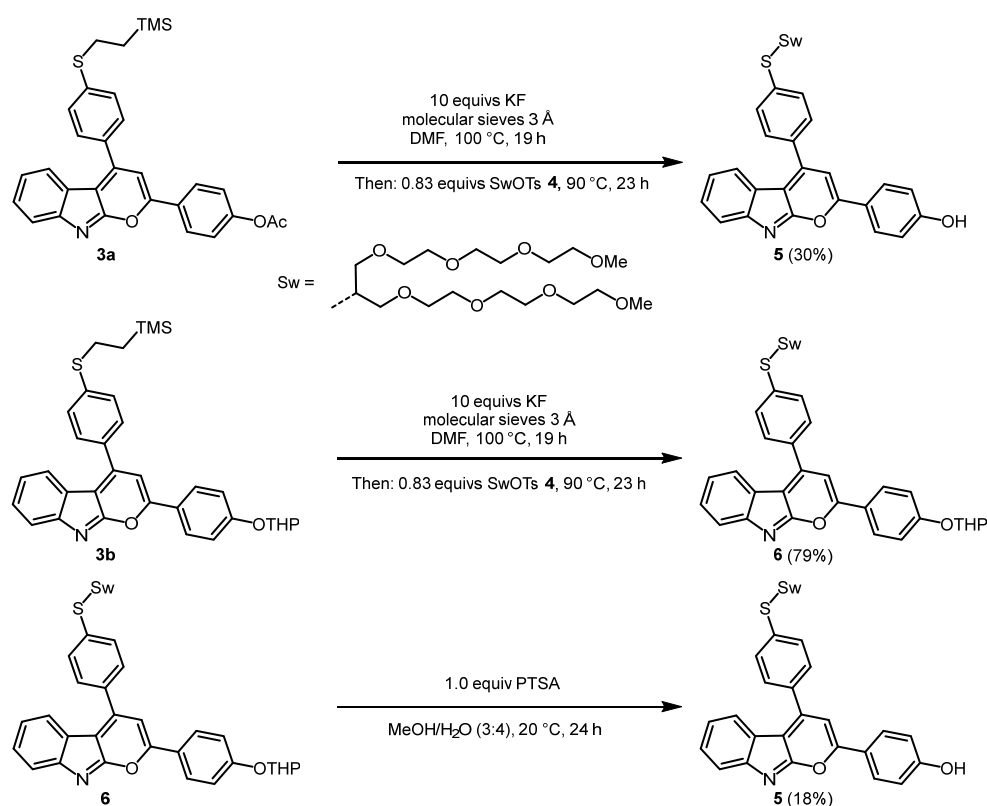### 2.1. Synthesis of the 2,4-diarylpyrano[2,3-b]indole Chromophores

Based on our previous synthetic protocols [61,62], a novel generation of halochromic 2,4-diarylpyrano[2,3-*b*]indoles containing a hydroxyl group has been created using our potassium fluoride mediated deprotection-alkylation one-pot reaction. Starting from secondary amide **1** [62] and terminal alkyne **2a** [63], the *O*-acyl protected 2,4-diarylpyrano[2,3-*b*]indole **3a** is formed by a Pd- and Cu-catalyzed domino insertion-coupling-cycloisomerization reaction in moderate yields of up to 54% (Scheme 2). Alternatively, 2,4-diarylpyrano[2,3-*b*]indole **3b** containing a 2-tetrahydropyranyl (THP) group can be synthesized by the coupling of alkyne **2b** in 73% yield.
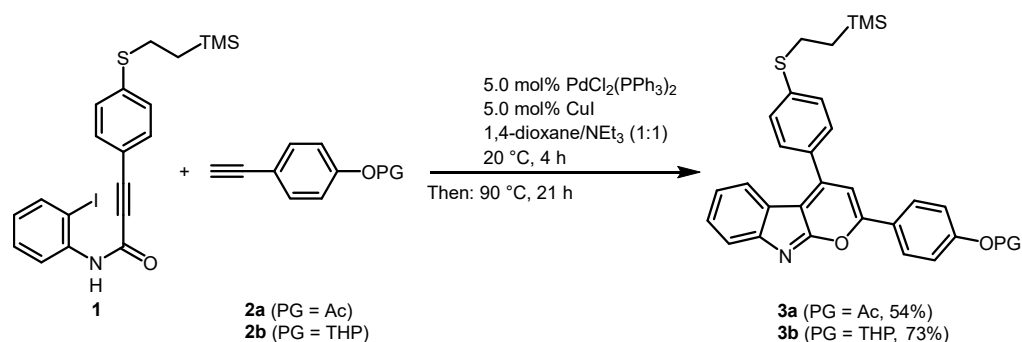
Scheme 2. Pd-Cu-catalyzed domino synthesis of *O*-protected 2,4-diarylpyrano[2,3-*b*]indoles **3**.

The solubilizing swallowtail substituent can be introduced by fluoride-induced desilylative cleavage of the (trimethylsilyl)ethyl group of 2,4-diarylpyrano[2,3-*b*]indoles **3** [62]. Interestingly, KF simultaneously acts as a desilylation and deacylation agent and for substrate **3a** (PG = Ac) both *O*- and *S*-protecting groups are concomitantly cleaved in the

presence of an excess of potassium fluoride and the subsequent addition of the swallowtail tosylate **4** selectively leads *S*-alkylation furnishing hydroxy 2,4-diarylpyrano[2,3-*b*]indole **5** in 30% yield in a one-pot fashion (Scheme 3). Activated molecular sieves, added at the beginning of the reaction, prove to be beneficial to maintain the thiolate intermediate, which is sensitive against moisture. In contrast, substrate **3b** (PG = THP) is transformed to the targeted hydroxy 2,4-diarylpyrano[2,3-*b*]indole **5** in two separate steps: first the desilylative *S*-alkylation with the swallowtail tosylate **4** in 79% yield and then a PTSA-mediated deprotective transacetalization [64] of the THP-protected *S*-alkyl derivative **6** furnishes the target compound **5** in 18% yield. Due to the lower overall yield of the last step, the first synthetic route starting from acyl-protected 2,4-diarylpyrano[2,3-*b*]indole **3a** is preferred. Also, this route is more elegant, since deprotection of the hydroxyl group takes place in the same reaction vessel. For further investigations, no distinctions were made between the products of the two different synthetic routes.


Scheme 3. Deprotection-alkylation synthesis of 2,4-diarylpyrano[2,3-*b*]indole **5** starting from substrates **3a** and **3b**.

Similarly as 2,4-diarylpyrano[2,3-*b*]indoles of the first [61] and second [62] generation, 2,4-diarylpyrano[2,3-*b*]indole **5** is also non-luminescent in the solid state and solution. Upon protonation with stronger acids, such as trifluoroacetic acid (TFA), solutions of 2,4-diarylpyrano[2,3-*b*]indole **5** exhibit yellow luminescence upon excitation with UV-light (Scheme 4, Figure 1 left). A similar effect was previously reported after adding metal cations, such as Zn^{2+} or Mg^{2+}, which are complexed by 2,4-diarylpyrano[2,3-*b*]indole **5** [61].

In addition, 2,4-diarylpyrano[2,3-*b*]indole **5** shows a peculiar response to deprotonation of the phenolic hydroxy group in solution with stronger bases, such as 1,8-diazabicyclo[5.4.0]undec-7-ene (DBU), which to this date has not been reported for this type of class. Upon deprotonation in solution, the resulting phenolate oxygen exerts a very strongly electron donating character, leading to an extended π-conjugated push-pull system displaying a bright red emission (Scheme 4, Figure 1 right). It is worthy of men-

tion, that both protonation and deprotonation are reversible upon the addition of TFA or DBU, respectively.
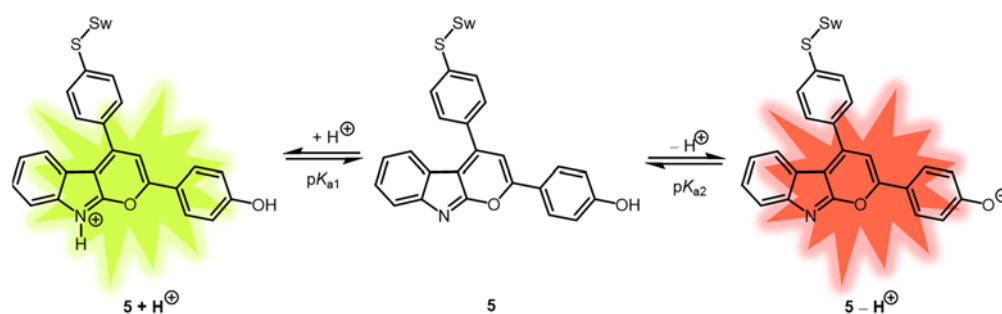
Scheme 4. Protonation (left) and deprotonation (right) of amphoteric 2,4-diarylpyrano[2,3-*b*]indole **5**.

Figure 1. Halochromic solutions ($c = 1.3 \times 10^{-3}$ mol·L^{-1}) of 2,4-diarylpyrano[2,3-*b*]indole **5** in propan-2-ol under daylight (top row) and UV-light (λ_{exc} = 354 nm) (bottom row). The solution protonated **5 + H$^+$** with TFA (left), the neutral solution of **5** (center), and the solution deprotonated **5 — H$^+$** with DBU (right).

2.2. Solubility of 2,4-diarylpyrano[2,3-b]indole 5

Next, the solubility of 2,4-diarylpyrano[2,3-*b*]indole **5** was scrutinized. Hereby, the focus was laid on identifying suitable solvents and solvent systems, where 2,4-diarylpyrano[2,3-*b*]indole **5** and its photophysical properties as well as other effects could be properly investigated.

Starting at a given concentration ($c = 1.3 \times 10^{-3}$ mol·L^{-1}), the mixture of 2,4-diarylpyrano[2,3-*b*]indole **5** and corresponding solvent were stirred for 30 min and sonicated for 10 min. Solubility upon eyesight was indicated with "+", whereas the presence of undissolved compound was indicated with "–". At first, organic solvents from lesser to higher polarity according to Reichardt's polarity scale [65] were employed (Table 1). Specifically, non-toxic solvents were of interest, opening the possibility for an application as a halochromic chemosensor for protons and the absence of such in biological systems.

As seen in Table 1, (un)branched alkanes like *n*-pentane and unbranched ethers like 2-methoxy-2-methylpropane (MTBE) are not suitable for solubilizing 2,4-diarylpyrano[2,3-*b*]indole **5**, whereas other non-polar solvents like benzene and toluene are able to dissolve 2,4-diarylpyrano[2,3-*b*]indole **5** completely. This can be plausibly rationalized by π-π interactions between molecules **5** and the aromatic solvent, preventing them from aggregation. More polar solvents, such as 1,4-dioxane, acetone, and propan-2-ol, are all suitable for further investigations, as well as chlorinated solvents, such as chloroform.

Table 1. Solubility screening of 2,4-diarylpyrano[2,3-*b*]indole **5** in different organic solvents ($c = 1.3 \times 10^{-3}$ mol·L^{-1}). Solvents were sorted with increasing polarity according to Reichardt's polarity scale [65].

Solvent	Solubility of Compound 5
cyclohexane	–
n-pentane	–
n-hexane	–
toluene	+
benzene	+
diethyl ether	–
methyl tert-butyl ether	–
1,4-dioxane	+
tetrahydrofuran	+
ethyl acetate	+
chloroform	+
dichloromethane	+
acetone	+
DMF	+
dimethyl sulfoxide	+
acetonitrile	+
propan-2-ol	+
ethanol	+
methanol	+
water	–

Most of the solvents able to dissolve chromophore **5** lead to intense luminescence after addition of an excess of TFA observed by the naked eye, but only a few solvents enable luminescence in the deprotonated state. Mainly protic solvents of higher polarity, such as propan-2-ol, ethanol or methanol, show noticeable luminescence, thus narrowing the applicable solvent spectrum for switching in the polarity range. For further photophysical investigations, propan-2-ol is employed as a protic solvent with the most intense luminescence in both protonated and deprotonated states for the naked eye.

Unfortunately, water alone, as the most polar protic solvent, is not able to solubilize chromophore **5**. Therefore, water mixtures with different polar co-solvents such as THF and propan-2-ol were prepared as well as selected aqueous systems and mixtures of compound **5** at different pH values (Table 2). Again, solubility at a specified concentration ($c = 1.3 \times 10^{-3}$ mol·L^{-1}) was indicated with "+", whereas the presence of undissolved compound was indicated with "–".

While biologically important buffers [66,67] like HEPES (2-[4-(2-hydroxyethyl)piperazin-1-yl]ethanesulfonic acid) or MOPS (3-morpholinopropane-1-sulfonic acid) did not facilitate the water solubility of dye **5**, a clear trend can be identified for aqueous systems at different pH values (Table 2). The more basic or acidic the solution, the better dye **5** is soluble. Below pH 3 and above pH 11, complete solubility was achieved. This can be rationalized by the structure and functional groups of 2,4-diarylpyrano[2,3-*b*]indole **5**. Below pH 3, complete protonation at the nitrogen atom of the indole moiety occurs and the positive charge causes repulsion and, hence, less π-π-stacking between the molecules and better solubility in aqueous media. The same principle holds true for aqueous solutions with pH >11. Through deprotonation with a strong organic base such as DBU, a phenolate is created, resulting in complete dissolving of dye **5** under these conditions. However, at higher pH values above 13, degradation of the 2,4-diarylpyrano[2,3-*b*]indoles can be observed [62]. Moreover, the pK_{a1} value for indole nitrogen atom protonation and the pK_{a2} value for phenol deprotonation can be estimated by the solubility. Since solubility starts below pH 3 and above pH 11, a pK_{a1} value of around 3 and pK_{a2} of around 11 can be roughly assumed. This qualitative estimation can be quantified by UV/Vis photometric determination of both pK_a values (see Section 2.4).

Table 2. Solubility screening of 2,4-diarylpyrano[2,3-*b*]indole **5** in different aqueous systems ($c = 1.3 \times 10^{-3}$ mol·L^{-1}).

Solvent	Solubility of Compound 5
water	−
buffer, HEPES, 0.1 mol·L^{-1}, pH 8	−
buffer, MOPS, 0.1 mol·L^{-1}, pH 7	−
water, HCl$_{(aq)}$, pH 1	+
water, HCl$_{(aq)}$, pH 3	−
water, pH 7	−
water, NaOH$_{(aq)}$, pH 11	−
water, NaOH$_{(aq)}$, pH 13	+
tetrahydrofuran/water	25:75
dimethyl sulfoxide/water	70:30
propan-2-ol/water	35:65

For the mixtures of organic co-solvent and water, 2,4-diarylpyrano[2,3-*b*]indole **5** is dissolved in each organic solvent and this solution is rapidly injected in the corresponding amount of water. In Table 2, the lowest amount of co-solvent, which is needed for solubilizing 2,4-diarylpyrano[2,3-*b*]indole **5** in aqueous media is presented. Hereby, the fraction of water is incrementally increased in steps of 5 vol-% until formation of clusters or turbid solutions can be observed indicating too high and non-suitable water fractions (Figure 2). At excessive fractions, the formation of clusters occurs rapidly just seconds after the mixing of the two solvents. Since we expect that size and appearance of the clusters depend strongly on the solvent mixture, we used dynamic light scattering (DLS) to analyze the different samples.

Figure 2. 2,4-Diarylpyrano[2,3-*b*]indole **5** in propan-2-ol with increasing water fractions from left (0%) and middle (70%) to right (95%). In the vial to the right cluster formation is clearly visible.

2.3. Particle size of 2,4-diarylpyrano[2,3-b]indole 5 in Aqueous Solutions

DLS was used to study the hydrodynamic size and size distribution with regard to the dependence of the water content in the solvent mixture. For this 2,4-diarylpyrano[2,3-*b*]indole **5** was dissolved in different propan-2-ol/water mixtures. The water content of the mixtures was varied from 75 up to 95 vol-% in 5 vol-% steps. All samples were sonicated for 30 min and filtered using a filter with 5 μm pore size before the DLS measurement. This was mostly done to remove dust and potentially very large impurities or aggregates. We want to highlight that the filtered samples did not show any precipitation in the course of several hours, i.e., much longer than the measurement times in DLS. The size distributions of all measured samples were obtained at a 110° scattering angle by CONTIN analysis [68] are shown in Figure 3.
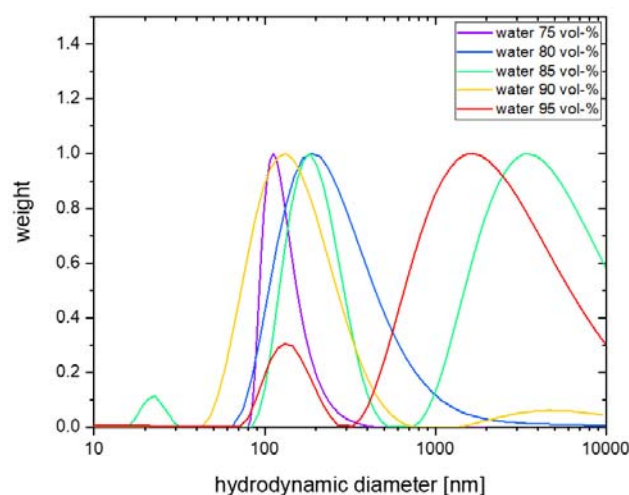
Figure 3. Size distribution of the 2,4-diarylpyrano[2,3-*b*]indole **5** cluster in different propan-2-ol water mixtures obtained from CONTIN analysis of DLS data.

At the lowest water concentration of 75 vol-% (purple) we find a monomodal size distribution with an average cluster size of approximately 140 nm in diameter. The narrow width of the distribution indicates rather low polydispersity. In contrast, when increasing the water content, the size distribution of the clusters shifts to larger sizes with increased polydispersity. For water contents of 85 vol-% and above, additional contributions become visible and the distribution functions become at least bimodal with a contribution from larger aggregates in the micrometer regime. Nevertheless, even these samples were found to be colloidally stable, at least in the course of hours. The size of the aggregates varies strongly between samples and cannot be precisely determined. In particular, the sample at a water concentration of 95 vol-% contains large and polydisperse aggregates that dominate the light scattering. This finding is in good agreement with our turbidity observations previously shown in this work. Nevertheless, we attempted analysis from angle-dependent DLS (see Figure S19, Supporting Information) to study the diffusive behavior of the smaller cluster phase. For these we find translational diffusion that allowed for a more quantitative size analysis. The results are reported in Table S3 (Supporting Information).

In addition, the stability of the clusters and aggregates over time was investigated. For this the measurements were repeated after one month. We found a significant increase in size and polydispersity after this aging time (see Figure S20, Supporting Information). This is a strong indication that the clusters are not stable in these solvent mixtures over a long period of time.

2.4. Photophysical Properties of 2,4-diarylpyrano[2,3-b]indole 5

Although non-luminescent in the solid state and in solution, 2,4-diarylpyrano[2,3-*b*]indole **5** displays peculiar luminescence under certain conditions, rendering it a turn-ON luminophore sensitive to acidic and basic solutions as well as for metal cations. Herein, the photophysical properties of 2,4-diarylpyrano[2,3-*b*]indole **5** in propan-2-ol under neutral, acidic, and basic conditions are discussed (Table 3, Figures 4 and 5).

In the ground state, the neutral dye **5** shows an expected absorption behavior comparable to 2,4-diarylpyrano[2,3-*b*]indoles with an 4-anisyl group at position 2 ($\lambda_{max,abs}$ = 369 nm) [62]. Upon protonation, the absorption maximum shifts from 372 to 455 nm. Moreover, the absorption maximum can be shifted even further bathochromically upon deprotonation, i.e., the absorption maximum is shifted from 372 to 533 nm. Instead of a cyanine chromophore in the acidic medium, an oxonol anion chromophore is formed in the basic medium. The molar decadic absorption coefficients ε of 2,4-diarylpyrano[2,3-*b*]indole **5** increase upon (de)protonation from 14,200 L·cm^{-1}·mol^{-1} for the neutral species **5** to 24,500 L·cm^{-1}·mol^{-1} for the deprotonated species **5 − H⁺** and 22,400 L·cm^{-1}·mol^{-1} for the protonated species **5 + H⁺**. Likewise, the emission maxima shift to longer wavelengths for the ionized forms

of 2,4-diarylpyrano[2,3-*b*]indole **5** with similar Stokes shifts of 3400 cm^{-1} (**5 + H$^+$**) and 2800 cm^{-1} (**5 − H$^+$**). The absolute quantum yields Φ_f for both species were measured with an Ulbricht sphere and reach up to Φ_f = 0.058 (**5 + H$^+$**) and Φ_f = 0.059 (**5 − H$^+$**).

Table 3. Photophysical data of 2,4-diarylpyrano[2,3-*b*]indole **5** recorded in propan-2-ol (c_0(**5**) = 10^{-5}–10^{-7} mol·L^{-1}) at *T* = 293 K. Protonated and deprotonated spectra were recorded with an excess amount of TFA or DBU (c(TFA/DBU) = 10^{-2} mol·L^{-1}).

Compound	$\lambda_{max,abs}$ [nm] (ε) [L·cm^{-1}·mol^{-1}]	$\lambda_{max,em}$ [nm]	*Stokes* Shift $\Delta\bar{\nu}$ [cm^{-1}]	Quantum Yield Φ_f
5	372 (14,200)	-	-	<0.010
5 + H$^+$ [a]	455 (22,400)	539	3400	0.039 [b] 0.058 [c]
5 − H$^+$ [a]	533 (24,500)	628	2800	0.059 [c]

[a] Protonation by addition of excess TFA or DBU (10 equivs). [b] Determined with Coumarin 153 in ethanol (Φ_f = 0.38) as standard [69]. [c] Absolute quantum yield.
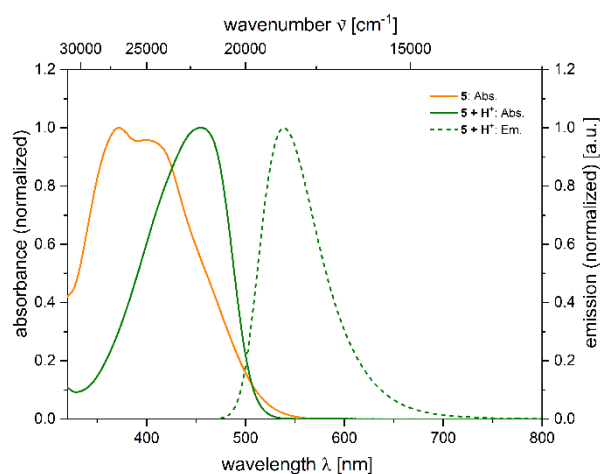

Figure 4. Normalized absorption spectrum of **5** (orange solid line), **5 + H$^+$** (green solid line), and normalized emission spectrum of **5 + H$^+$** (green dashed line) (c_0(**5**) = 5.0 × 10^{-5} mol·L^{-1}, c(TFA) = 10^{-2} mol·L^{-1}, recorded in propan-2-ol at *T* = 293 K, $\lambda_{exc,\mathbf{5 + H}^+}$ = 455 nm).
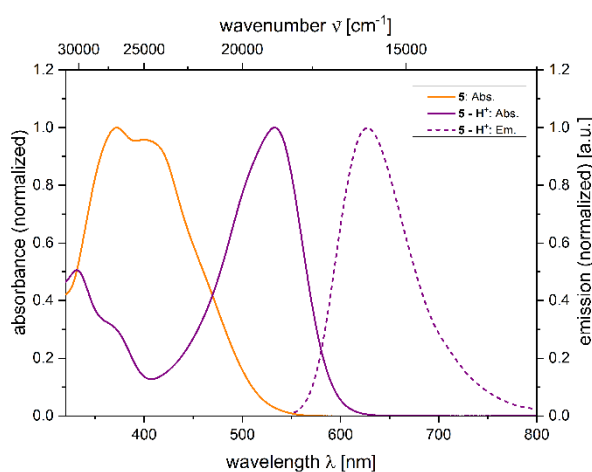

Figure 5. Normalized absorption spectrum of **5** (orange solid line), **5 − H$^+$** (purple solid line), and normalized emission spectrum of **5 − H$^+$** (purple dashed line) (c_0(**5**) = 5.0 × 10^{-5} mol·L^{-1}, c(DBU) = 10^{-2} mol·L^{-1}, recorded in propan-2-ol at *T* = 293 K, $\lambda_{exc,\mathbf{5 - H}^+}$ = 533 nm).

As seen in Table 2, 2,4-diarylpyrano[2,3-*b*]indole **5** is soluble in mixtures of water and propan-2-ol up to 65:35 vol-%, raising the question, how the photophysical properties are

affected by water as a solvent. After replacing about 2/3 of the organic solvent by water, molar decadic absorption coefficients ε for all 2,4-diarylpyrano[2,3-*b*]indole species **5**, **5 + H⁺**, and **5 − H⁺** increase up to 70% (Table 4).

Table 4. Photophysical data of 2,4-diarylpyrano[2,3-*b*]indole **5**, **5 + H⁺**, and **5 − H⁺** recorded in propan-2-ol/water ($c_0(\mathbf{5}) = 10^{-5}$–$10^{-7}$ mol·L^{-1}) at T = 293 K. Protonated and deprotonated spectra were recorded with an excess amount of TFA or DBU (c(TFA/DBU) = 10^{-2} mol·L^{-1}).

Compound	$\lambda_{max,abs}$ [nm] (ε) [L·cm^{-1}·mol^{-1}]	$\lambda_{max,em}$[nm]	*Stokes* Shift $\Delta \bar{v}$ [cm^{-1}]	Quantum Yield Φ_f
5	373 (24200)	-	-	<0.010
5 + H⁺ [a]	447 (37900)	543	4000	0.014 [b]
5 − H⁺ [a]	509 (34500)	624	3600	0.018 [b]

[a] Protonation by addition of excess TFA or DBU (10 equivs). [b] Absolute quantum yield.

While emission bands of **5 + H⁺** and **5 − H⁺** remain at the same wavelength as in pure propan-2-ol (Figures 6 and 7), absorption bands are slightly shifted hypsochromically, resulting in larger Stokes shifts up to $\Delta \bar{v}$ = 4000 cm^{-1}. Expectedly, the absolute quantum yields of **5 + H⁺**, and **5 − H⁺** diminish and amount to Φ_f = 0.014 and Φ_f = 0.018, respectively, in propan-2-ol/water (35:65). Above a water fraction of 65%, formation of clusters can be observed leading to poorly resolved and noisy UV/Vis spectra.
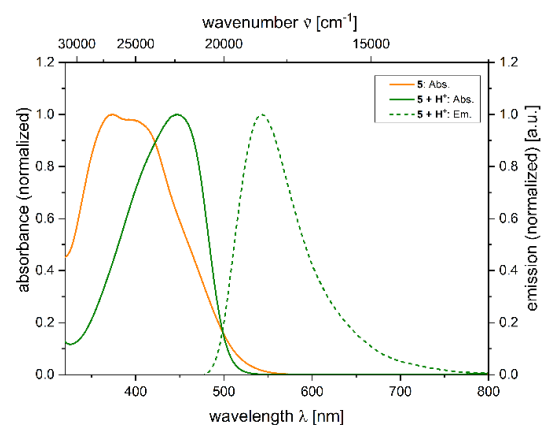

Figure 6. Normalized absorption spectra of **5** (orange solid line), **5 + H⁺** (green solid line), and normalized emission spectrum of **5 + H⁺** (green dashed line) ($c_0(\mathbf{5})$ = 5.1 × 10^{-5} mol·L^{-1}, recorded in propan-2-ol/H$_2$O (35:65) at T = 293 K; $\lambda_{\mathrm{exc},\mathbf{5+H^+}}$ = 447 nm).
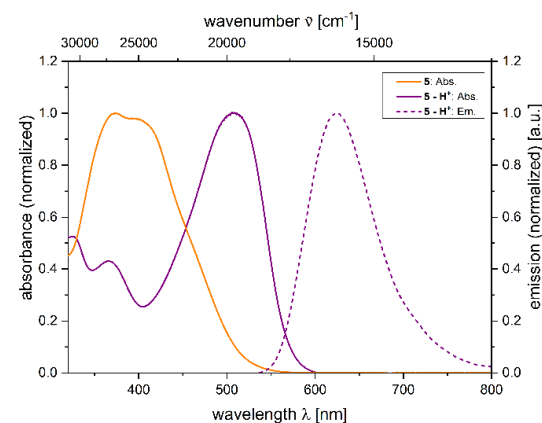

Figure 7. Normalized absorption spectra of **5** (orange solid line), **5 − H⁺** (purple solid line), and normalized emission spectrum of **5 − H⁺** (purple dashed line) ($c_0(\mathbf{5})$ = 5.1 × 10^{-5} mol·L^{-1}, recorded in propan-2-ol/H$_2$O (35:65) at T = 293 K; $\lambda_{\mathrm{exc},\mathbf{5-H^+}}$ = 509 nm).

For chemosensors, the analyte as well as the spectrum of action are essential and define their possible application. In the case of 2,4-diarylpyrano[2,3-*b*]indole **5**, besides metal cations, the main analytes are acidic and basic solutions due to its amphiprotic character. For amphiprotic molecules, the spectrum of action is defined by its two pK_a values, which can be determined by UV/Vis absorption titration and their change can be monitored in the presence of an analyte.

For the determination of pK_{a1} of 2,4-diarylpyrano[2,3-*b*]indole **5**, absorption spectra at various pH values in a range from 7 to 1.3 can be recorded upon addition of TFA in propan-2-ol. Propan-2-ol as a solvent is completely miscible with both TFA and DBU and the spectra are less noisy in comparison to other solvents, such as THF. In addition, propan-2-ol/water is also an aqueous system, where 2,4-diarylpyrano[2,3-*b*]indole **5** is soluble and, thus, can be employed as chemosensor.

The spectra at different pH values display isosbestic points, indicating that deprotonation proceeds directly without an intermediate (Figure 8) [70]. The involved species are **5** and **5 + H⁺** furnishing a pK_{a1} value of 3.5 for the deprotonation of **5 + H⁺** (for details, see Supporting Information).
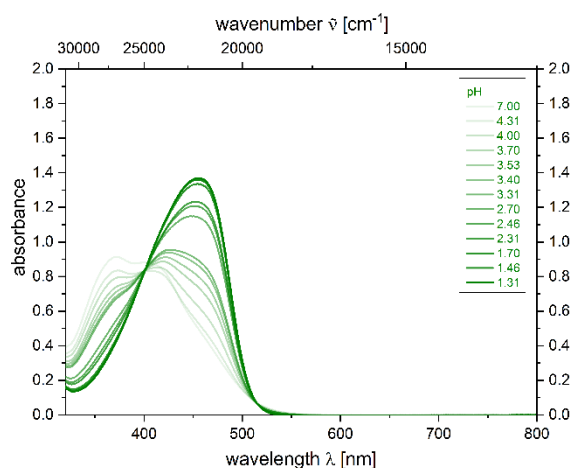

Figure 8. Absorption spectra of **5** (c_0(**5**) = 5.0×10^{-5} mol·L^{-1}) at different concentrations of trifluoroacetic acid (recorded in propan-2-ol at T = 293 K).

Likewise, the pK_{a2} value of the phenolic hydroxy group can be determined by titration with DBU as a base. Again, the occurrence of isosbestic points indicates the direct transition from species **5** to **5 − H⁺** without an intermediate (Figure 9) furnishing the corresponding pK_a value of 10.5 for the deprotonation of **5** (for details, see Supporting Information). The average of both pK_a values accounts for an isoelectric point of pH = 7 for compound **5**. The calculated isoelectric point is in agreement with previous observations that neutral 2,4-diarylpyrano[2,3-*b*]indole **5** is insoluble in water at this pH region and facilitates aggregation.

Furthermore, the emission properties at different pH values can be investigated. Upon titration, the pH detection limit under acidic and basic conditions is first determined (Figures 10 and 11). For the addition of TFA, luminescence is turned on at pH values smaller than 5.31, as for the addition of DBU, luminescence turns on at pH values higher than 8.70. This leads to a blind spot of the chemosensor **5** between pH 5.31–8.70, where no significant emission takes place.

Finally, the proper reversibility after binding an analyte and, thus, the accuracy of the results have to be ascertained. For 2,4-diarylpyrano[2,3-*b*]indole **5**, the reversibility is tested by an alternating addition of an excess amount of TFA and DBU to a neutral solution of 2,4-diarylpyrano[2,3-*b*]indole **5** in propan-2-ol. After the first cycle of addition of TFA, DBU, and again TFA to 2,4-diarylpyrano[2,3-*b*]indole **5**, a decrease in absorbance can be seen (Figure 12), probably due to ion strength of [DBU-H⁺][TFA⁻] and its interaction with the chromophore. Furthermore, a comparably smaller decrease in absorbance after each

cycle can be attributed to dilution by increasing the amount of acid and base, respectively. The color change during these cycles occurs considerably fast, allowing a rapid readout just in seconds after addition of the analyte. After five cycles, no further effects besides small decreases in absorbance can be seen and, therefore, a good reversibility of this chemosensor can be concluded.
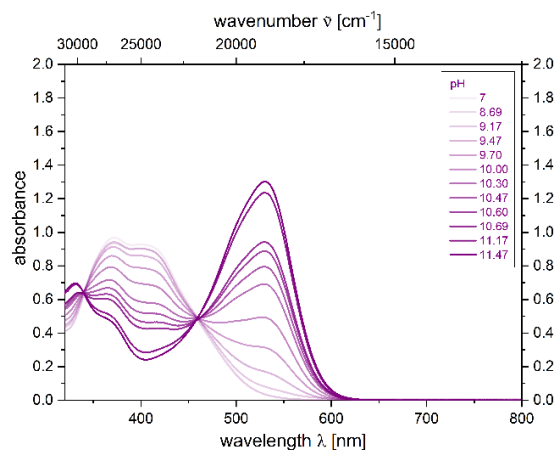

Figure 9. Absorption spectra of **5** (c_0(**5**) = 5.0 × 10^{-5} mol·L^{-1}) at different concentrations of 1,8-diazabicyclo[5.4.0]undec-7-ene (DBU) (recorded in propan-2-ol at *T* = 293 K).

Figure 10. Emission spectra of **5** (c_0(**5**) = 5.0 × 10^{-5} mol·L^{-1}) at different concentrations of trifluoroacetic acid (recorded in propan-2-ol at *T* = 293 K).
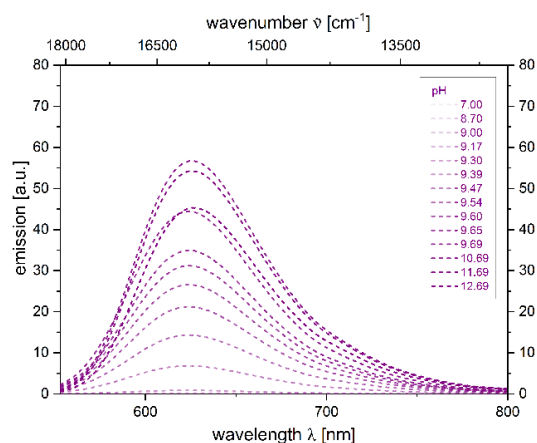
Figure 11. Emission spectra of **5** (c_0(**5**) = 5.0 × 10^{-5} mol·L^{-1}) at different concentrations of 1,8-diazabicyclo[5.4.0]undec-7-ene (DBU) (recorded in propan-2-ol at *T* = 293 K).

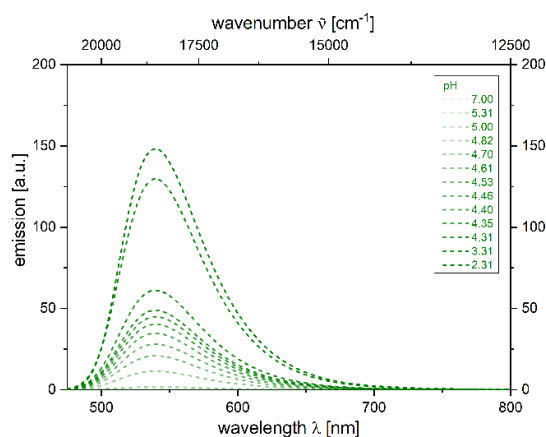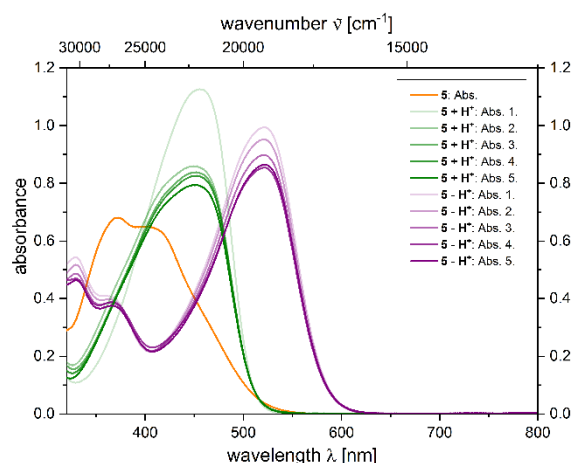**Figure 12.** Absorption spectra of **5** (c_0(**5**) = 3.5 × 10^{-5} mol·L^{-1}, pH = 1.5–12.5) after alternating addition of trifluoroacetic acid and 1,8-diazabicyclo[5.4.0]undec-7-ene (DBU) (recorded in propan-2-ol at *T* = 293 K).

3. Materials and Methods

3.1. General Considerations

Commercially available chemicals were purchased reagent grade and used without further purification. *N*-(2-iodophenyl)-3-(4-((2-(trimethylsilyl)ethyl)thio)phenyl)propiolamide (**1**) [62], 4-ethynylphenyl acetate (**2**) [63,71,72], swallowtail-tosylate (Sw-OTs, **4**) [71–73], and 2-(4-ethynylphenoxy)tetrahydro-2*H*-pyran (**6**) [74,75], were prepared according to literature protocols. Reactions were performed in oven-dried Schlenk tubes under a nitrogen atmosphere unless stated otherwise. Dry solvents were dried through a solvent purification system (MB-SPS-800, M. Braun Inertgas-Systeme, Garching, Germany). Reaction progress was qualitatively monitored using silica gel layered aluminium foil (60 F_{254}, Merck, Kenilworth, NJ, USA). For detection, UV light of wavelengths 254 nm and 365 nm as well as an aqueous potassium permanganate solution was used. Column chromatography was performed using flash technique under pressure of 2 bar with silica gel 60, mesh 230-400 (Macherey-Nagel, Düren, Germany). ^{1}H and ^{13}C NMR spectra were measured on an Avance III-300 (Bruker, Billerica, MA, USA) and Avance III-600 (Bruker, Billerica, MA, USA) spectrometer. Chemical shifts (δ) were referenced to the internal solvent signal: $CDCl_3$ (^{1}H δ 7.26, ^{13}C δ 77.2). Multiplicities are stated as: s (singlet), d (doublet), dd (doublet of doublet), t (triplet), and m (multiplet). Coupling constants (*J*) are given in Hz. The assignment of primary (CH_3), secondary (CH_2), tertiary (CH) and quaternary carbon nuclei (C_{quat}) was made using DEPT-135 spectra. Mass spectrometric investigations were carried out at the Department of Mass Spectrometry of the Institute of Inorganic and Structural Chemistry, Heinrich-Heine-Universität Düsseldorf. IR spectra were recorded using an IR Affinity-1 spectrometer (Shimadzu, Kyoto, Japan) via the attenuated total reflection (ATR) method. The intensities of the IR bands are abbreviated as w (weak), m (medium), s (strong). Melting points (uncorrected) were measured using a Melting Point B-540 (Büchi, Oldham, UK). Combustion analyses were measured on a Series II Analyser 2400 (Perkin Elmer, Waltham, MA, USA) at the Institute of Pharmaceutical and Medicinal Chemistry, Heinrich-Heine-Universität Düsseldorf. Absorption spectra were recorded on a UV/Vis/NIR Lambda 19 spectrometer (Perkin Elmer, Waltham, MA, USA). Molar extinction coefficients ε were determined by absorption measurements at five different concentrations. Emission spectra were recorded using a F-7000 spectrometer (Hitachi, Tokyo, Japan) and corrected with spectra of the solvent mixtures. Excitation slit was set to 5.0 nm and emission slit was set to 10 nm. PMT Voltage was set to 350 V and scan speed was set to 240 nm/min. Absolute quantum yields were determined using a Spectrofluorometer FS5 (Edinburgh Instruments, Livingston, UK). Light scattering experiments were performed on a 3D LS Spectrometer (LS Instruments, Fribourg, Switzerland) in 2D mode. A HeNe-Laser was used as a light source

and two Avalanche photodiodes in cross-correlation mode were used for the detection of scattered light. The samples were placed in a refractive index matching bath filled with decalin. The temperature control was realized with a JULABO CF31 and a PT100 probe near the sample position. The samples were prepared in Fisherbrand culture tubes (Fisher Scientific GmbH, Schwerte, Germany) with an outer diameter of 1 cm. Measurements were performed over a range of scattering angles of 30° to 140° in 10° steps. Three measurements with acquisition times between 10 and 60 s, depending on the scattering intensity of the sample, were performed at each angle. The temperature for all measurements was set to 25 °C. The data were analyzed using the CONTIN algorithm [68] as implemented in AfterALV v.1.0e (Dullware), The Netherlands.

3.2. Synthesis of 4-(4-(4-((2-(trimethylsilyl)ethyl)thio)phenyl)pyrano[2,3-b]indol-2-yl)phenyl acetate (**3a**)

To a degassed solution of **1** (1.38 g, 2.88 mmol) in triethylamine/1,4-dioxane (1:1, 28 mL) was added $PdCl_2(PPh_3)_2$ (0.101 g, 0.144 mmol), CuI (0.027 g, 0.14 mmol), and alkyne **2a** (0.508 g, 3.17 mmol) and the mixture was stirred at 20 °C for 4 h. Then, the reaction mixture was stirred at 90 °C for another 18 h. After cooling to room temp, the mixture was diluted with water (50 mL) and extracted with ethyl acetate (3 × 100 mL). The combined organic layers were then washed with a saturated solution of aqueous NH_4Cl (2 × 100 mL) and dried with anhydrous Na_2SO_4. After filtration, the solvent was removed under reduced pressure and the crude product was purified by column chromatography on silica gel (cyclohexane/ethyl acetate (1:1)) and recrystallized in *n*-hexane/ethyl acetate (3:1) to give compound **3a** (0.815 g, 1.59 mmol, 54%) as a dark red solid, Mp 90 °C. R_f (*n*-hexane/acetone 1:1) = 0.30.

^{1}H NMR (300 MHz, CDCl$_3$): δ 0.11 (s, 9 H), 1.01–1.07 (m, 2 H), 2.35 (s, 3 H), 3.08–3.14 (m, 2 H), 7.11–7.16 (m, 2 H), 7.29 (d, $^3J_{H-H}$ = 8.7 Hz, 2 H), 7.47–7.52 (m, 3 H), 7.73–7.81 (m, 4 H), 8.10 (d, $^3J_{H-H}$ = 8.7 Hz, 2 H). ^{13}C NMR (75 MHz, CDCl$_3$): δ −1.6 (CH$_3$), 16.7 (CH$_2$), 21.3 (CH$_3$), 28.7 (CH$_2$), 104.8 (CH), 118.7 (C$_{quat}$), 119.3 (CH), 121.8 (CH), 122.4 (CH), 122.5 (C$_{quat}$), 122.6 (CH), 127.5 (CH), 127.8 (CH), 129.0 (CH), 129.3 (CH), 129.3 (C$_{quat}$), 132.9 (C$_{quat}$), 141.9 (C$_{quat}$), 146.6 (C$_{quat}$), 151.6 (C$_{quat}$), 152.9 (C$_{quat}$), 155.4 (C$_{quat}$), 165.1 (C$_{quat}$), 169.1 (C$_{quat}$). IR (ATR): $\tilde{v}$ [cm^{-1}] 2951 (w), 1755 (m), 1636 (m), 1593 (w), 1541 (m), 1522 (s), 1503 (s), 1472 (m), 1437 (m), 1414 (m), 1368 (m), 1321 (w), 1302 (w), 1281 (w), 1256 (w), 1246 (m), 1188 (s), 1165 (s), 1125 (m), 1109 (m), 1098 (m), 1086 (m), 1070 (m), 1043 (w), 1013 (m), 976 (m), 951 (w), 910 (m), 883 (w), 837 (s), 818 (s), 799 (m), 775 (m), 756 (s), 731 (s), 718 (m), 704 (m), 692 (m), 673 (m), 656 (m), 604 (m). HR-MS (ESI) calcd. for [C$_{30}$H$_{29}$NO$_3$SSi + H]$^+$: 512.1637; Found: 512.1719. Anal. calcd. for C$_{30}$H$_{29}$NO$_3$SSi [511.71]: C 70.42, H 5.71, N 2.74, S 6.27; Found: C 70.22, H 5.79, N 2.70, S 6.20.

3.3. Synthesis of 2-(4-((tetrahydro-2H-pyran-2-yl)oxy)phenyl)-4-(4-((2-(trimethylsilyl)ethyl)-thio)phenyl)pyrano[2,3-b]indole (**3b**)

To a degassed solution of **1** (0.24 g, 0.50 mmol) in triethylamine/1,4-dioxane (1:1, 5 mL) was added $PdCl_2(PPh_3)_2$ (0.018 g, 0.025 mmol), CuI (0.0048 g, 0.025 mmol), and alkyne **2b** (0.111 g, 0.550 mmol) and the mixture was stirred at 20 °C for 4 h. Then, the reaction mixture was stirred at 90 °C for another 18 h. After cooling to room temp the mixture was diluted with water (50 mL) and extracted with ethyl acetate (4 × 50 mL). The combined organic layers were then washed with a saturated solution of aqueous NH_4Cl (2 × 100 mL) and dried with anhydrous Na_2SO_4. After filtration, the solvent was removed under reduced pressure and the crude product was purified by column chromatography on silica gel (cyclohexane/ethyl acetate (1:1)) and recrystallized in *n*-hexane/ethyl acetate (3:1) to give compound **3b** (0.201 g, 0.363 mmol, 73%) as an orange solid, Mp 135 °C. R_f (*n*-hexane/ethyl acetate (1:1)): 0.36.

^{1}H NMR (300 MHz, CDCl$_3$): δ 0.11 (s, 9 H), 1.01–1.07 (m, 2 H), 1.60–1.79 (m, 3 H), 1.88–1.95 (m, 2 H), 1.97–2.08 (m, 1 H), 3.08–3.13 (m, 2 H), 3.62–3.69 (m, 1 H), 3.85–3.94 (m, 1 H), 5.53 (t, $^3J_{H-H}$ = 2.8 Hz, 1 H), 7.07–7.14 (m, 2 H), 7.17–7.20 (m, 2 H), 7.44–7.50 (m, 3 H), 7.72–7.78 (m, 4 H), 8.02 (d, $^3J_{H-H}$ = 8.7 Hz, 2 H). ^{13}C NMR (75 MHz, CDCl$_3$): δ 1.5 (CH$_3$), 16.9

(C$_{quat}$), 18.8 (CH$_2$), 25.3 (CH$_2$), 29.0 (CH$_2$), 30.0 (CH$_2$), 62.3 (CH$_2$), 80.0 (CH), 97.0 (C$_{quat}$), 103.7 (CH$_2$), 117.2 (CH), 119.3 (CH), 121.6 (CH), 122.3 (CH), 122.6 (CH), 123.0 (C$_{quat}$), 125.0 (CH), 127.9 (CH), 128.1 (C$_{quat}$), 129.0 (CH), 129.1 (CH), 133.4 (C$_{quat}$), 141.7 (C$_{quat}$), 156.8 (C$_{quat}$), 159.9 (C$_{quat}$), 170.9 (C$_{quat}$), 173.3 (C$_{quat}$). IR (ATR): $\tilde{v}$ [cm^{-1}] 3046 (w), 2941 (w), 2922 (w), 2852 (w), 1632 (m), 1607 (w), 1593 (m), 1522 (s), 1504 (s), 1468 (m), 1441 (s), 1422 (s), 1379 (m), 1346 (w), 1327 (w), 1285 (w), 1240 (s), 1196 (m), 1177 (m), 1146 (w), 1128 (w), 1101 (m), 1072 (m), 1063 (m), 1032 (s), 1007 (m), 957 (w), 939 (w), 920 (w), 905 (w), 876 (m), 858 (m), 820 (s), 806 (m), 777 (m), 760 (s), 750 (m), 721 (m), 706 (m), 694 (m), 677 (w), 640 (w), 613 (m). HR-MS (ESI) calcd. for [C$_{33}$H$_{35}$NO$_3$SSi + H]$^+$: 554.2107; Found: 554.2180. Anal. calcd. for C$_{33}$H$_{35}$NO$_3$SSi [553.79]: C 71.57, H 6.37, N 2.53, S 5.79; Found: C 71.65, H 6.39, N 2.58, S 5.84.

*3.4. Synthesis of 4-(4-(4-((2,5,8,11,15,18,21,24-octaoxapentacosan-13-yl)thio)phenyl)-pyrano[2,3-b]indol-2-yl)phenol (**5**)*

A mixture of **3a** (0.760 g, 1.49 mmol), KF (0.720 g, 12.4 mmol) and molecular sieves (15 pellets, 3 Å) in dry DMF (19 mL) was stirred at 100 °C for 19 h. After cooling to room temp, **4** (0.667 g, 1.24 mmol) was added and the suspension was stirred at 90 °C for 23 h. After cooling to room temp, water (30 mL) was added, and the mixture was filtrated and rinsed with ethyl acetate (50 mL). The aqueous layer was extracted with ethyl acetate (3 × 150 mL). The combined organic layers were washed with brine (150 mL) and dried with anhydrous Na$_2$SO$_4$. After filtration, the solvent was removed under reduced pressure and the crude product was purified twice by column chromatography on silica gel (petroleum ether/dichloromethane/ethyl acetate/methanol (5:3:1:0.3 to 5:3:1:0.9)) to give compound **5** (0.270 g, 0.367 mmol, 30%) as a red oil. R$_f$ (dichloromethane/methanol (20:1)): 0.45.

^{1}H NMR (300 MHz, CDCl$_3$): δ 2.08 (s, 1 H), 3.36 (s, 6 H), 3.52–3.55 (m, 4 H), 3.65–3.69 (m, 21 H), 3.79–3.81 (m, 4 H), 7.18 (t, $^3J_{H\text{-}H}$ = 7.7 Hz, 2 H), 7.34 (d, $^3J_{H\text{-}H}$ = 8.6 Hz, 2 H), 7.49 (t, $^3J_{H\text{-}H}$ = 7.7 Hz, 1 H), 7.66 (d, $^3J_{H\text{-}H}$ = 8.2 Hz, 2 H), 7.76-7.80 (m, 2 H), 7.90 (d, $^3J_{H\text{-}H}$ = 8.6 Hz, 2 H). ^{13}C NMR (75 MHz, CDCl$_3$): δ 1.2 (CH$_2$), 29.8 (CH$_3$), 47.6 (CH$_2$), 59.2 (CH$_2$), 70.6 (CH), 70.7 (CH), 70.8 (CH), 70.8 (CH), 70.9 (CH), 71.0 (CH), 72.1 (CH), 103.8 (CH$_2$), 116.2 (C$_{quat}$), 117.4 (CH$_2$), 118.3 (CH$_2$), 121.9 (C$_{quat}$), 122.0 (CH), 122.2 (C$_{quat}$), 122.3 (CH), 128.7 (CH$_2$), 128.9 (CH), 129.2 (C$_{quat}$), 130.2 (C$_{quat}$), 134.0 (C$_{quat}$), 139.9 (C$_{quat}$), 149.1 (C$_{quat}$), 158.3 (C$_{quat}$), 161.8 (C$_{quat}$). IR (ATR): $\tilde{v}$ [cm^{-1}] 3138 (w), 3076 (w), 2871 (m), 2814 (w), 2683 (w), 2598 (w), 2490 (w), 2423 (w), 1632 (m), 1605 (m), 1589 (m), 1574 (w), 1526 (m), 1506 (m), 1468 (m), 1441 (m), 1429 (m), 1379 (m), 1352 (w), 1327 (w), 1288 (m), 1242 (m), 1211 (w), 1196 (m), 1177 (s), 1099 (s), 1086 (s), 1028 (m), 1015 (m), 978 (m), 957 (m), 934 (w), 864 (w), 820 (m), 775 (m), 756 (m), 741 (w), 719 (w), 704 (m), 675 (w), 660 (w), 642 (w), 629 (w). HR-MS (ESI) calcd. for [C$_{40}$H$_{49}$NO$_{10}$S] + H$^+$: 736.3150; Found: 736.3152. Anal. calcd. for C$_{40}$H$_{49}$NO$_{10}$S [735.89]: C 65.29, H 6.71, N 1.90, S 4.36; Found: C 65.01, H 6.31, N 1.87, S 3.98.

*3.5. Synthesis of 4-(4-((2,5,8,11,15,18,21,24-octaoxapentacosan-13-yl)thio)phenyl)-2-(4-((tetrahydro-2H-pyran-2-yl)oxy)phenyl)pyrano[2,3-b]indole (**6**)*

A mixture of **3b** (0.614 g, 1.20 mmol), KF (0.720 g, 12.4 mmol) and molecular sieves (15 pellets, 3 Å) in dry DMF (15 mL) was stirred at 100 °C for 19 h. After cooling to room temp, **4** (0.581 g, 10.0 mmol) was added and the suspension was stirred at 90 °C for 23 h. After cooling to room temp again, water (30 mL) was added, and the mixture was filtrated and rinsed with ethyl acetate (50 mL). The aqueous layer was extracted with ethyl acetate (3 × 150 mL). The combined organic layers were washed with brine (150 mL) and dried with anhydrous Na$_2$SO$_4$. After filtration, the solvent was removed under reduced pressure and the crude product was purified twice by column chromatography on silica gel (petroleum ether/dichloromethane/ethyl acetate/methanol (5:3:1:0.3 to 5:3:1:0.9)) to give compound **6** (0.645 g, 0.786 mmol, 79%) as a red oil. R$_f$ (petroleum ether/ethyl acetate/dichloromethane/methanol (5:3:1:0.3)): 0.48.

^{1}H NMR (600 MHz, CDCl$_3$): δ 1.66–1.74 (m, 3 H), 1.88–1.92 (m, 2 H), 2.00–2.04 (m, 1 H), 3.37 (s, 6 H), 3.52–3.54 (m, 4 H), 3.62–3.68 (m, 21 H), 3.78–3.82 (m, 4 H), 3.84–3.87 (m, 1 H), 3.88–3.90 (m, 1 H), 5.54 (t, $^3J_{H-H}$ = 2.8 Hz, 1 H), 7.13 (t, $^3J_{H-H}$ = 6.0 Hz, 1 H), 7.19 (d, $^3J_{H-H}$ = 9.4 Hz, 1 H), 7.32 (d, $^3J_{H-H}$ = 7.9 Hz, 2 H), 7.49 (t, $^3J_{H-H}$ = 7.5 Hz, 1 H), 7.64 (d, $^3J_{H-H}$ = 8.5 Hz, 2 H), 7.73–7.76 (m, 2 H), 7.81 (d, $^3J_{H-H}$ = 8.3 Hz, 2 H), 8.04 (d, $^3J_{H-H}$ = 8.9 Hz, 2 H). IR (ATR): $\tilde{v}$ [cm^{-1}] 3049 (w), 2938 (w), 2868 (w), 1697 (w),1634 (m), 1603 (m), 1541 (m),1526 (m), 1504 (s), 1468 (m), 1439 (m), 1422 (m), 1371 (m), 1356 (m), 1323 (w), 1283 (m), 1240 (s), 1194 (m), 1177 (s), 1098 (s), 1049 (m), 1036 (s), 1022 (m), 955 (s), 916 (s), 872 (m), 820 (s), 777 (m), 758 (m), 735 (m), 704 (m), 640 (m). HR-MS (ESI) calcd. for [C$_{45}$H$_{57}$NO$_{11}$S + H]$^+$: 820.3725; Found: 820.3726. Anal. calcd. for C$_{45}$H$_{57}$NO$_{11}$S [819.37]: C 65.91, H 7.01, N 1.71, S 3.91; Found: C 66.06, H 6.53, N 1.79, S 4.22.

3.6. Alternative Synthesis of 4-(4-(4-((2,5,8,11,15,18,21,24-octaoxapentacosan-13-yl)thio)phenyl)-pyrano[2,3-b]indol-2-yl)phenol (**5**)

A mixture of **6** (0.840 g, 1.02 mmol) and PTSA monohydrate (0.019 g, 1.02 mmol) in methanol (1.5 mL) and water (2.0 mL) was stirred at room temp for 24 h. Afterwards, dichloromethane (50 mL) was added, and the mixture was washed with a saturated solution of NaHCO$_3$ (2 × 100 mL). The aqueous layers were combined and extracted with dichloromethane (2 × 100 mL). Subsequently, the organic layers were combined, washed with brine (100 mL), and dried with anhydrous Na$_2$SO$_4$. After filtration, the solvent was removed under reduced pressure and the crude product was purified twice by column chromatography on silica gel (petroleum ether/dichloromethane/ethyl acetate/methanol (5:3:1:0.3 to 5:3:1:0.9)) to give compound **5** (0.136 g, 0.186 mmol, 18%) as a red oil.

The NMR data were identical with the sample prepared under Section 3.4.

4. Conclusions

The Pd/Cu-catalyzed domino insertion-coupling-cycloisomerization of alkynoyl *o*-iodo anilides and terminal arylacetylenes furnishes a novel 2,4-diarylpyrano[2,3-*b*]indole, which is employed as a substrate for the preparation of a versatile amphiprotic turn-ON luminophore using a fluoride mediated double deprotection-alkylation process in a one-pot fashion. Solubility screenings reveal that the chemosensor can be used in most of organic solvents including DMSO, propan-2-ol and ethanol. Furthermore, aqueous mixtures of up to a 75:25 vol-% water-co-solvent ratio are accessible. The photophysical properties of this hydroxy-2,4-diarylpyrano[2,3-*b*]indole are dependent on the pH of the solvent system. Here, yellow or red luminescence is turned on under acid or basic conditions, respectively, allowing a sensitive read-out against a dark background and a reversible fine tuning of the absorption and emission characteristics. As an improvement over the previous second generation of 2,4-diarylpyrano[2,3-*b*]indoles, higher quantum yields of up to Φ_f = 0.058 and Φ_f = 0.059 in propan-2-ol for the protonated and deprotonated species respectively have been detected. In an aqueous mixture of 75:25 vol-% water/co-solvent ratio, clusters of approximately 140 nm in diameter are formed. These clusters start to rapidly form aggregates at higher concentrations of water. Further studies on the formation of clusters in solution as well as their application in biological systems are currently underway.

References

1. Müller, T.J.J.; Bunz, U.H.F. (Eds.) *Functional Organic Materials*; Wiley-VHC: Weinheim, Germany, 2007. [CrossRef]
2. Xie, L.; Tang, W.; Liu, Z.; Tang, W.; Yuan, Z.; Qin, Y.; Yan, L.; Zhu, X.; Zhu, W.; Wang, X. Effects of side-chain engineering with the S Atom in Thieno3,2-bthiophene-porphyrin to obtain small-molecule donor materials for organic solar cells. *Molecules* **2021**, *26*, 6134. [CrossRef] [PubMed]
3. Braveenth, R.; Bae, I.-J.; Han, J.-H.; Qiong, W.; Seon, G.; Raagulan, K.; Yang, K.; Park, Y.H.; Kim, M.; Chai, K.Y. Utilizing a spiro core with acridine-and phenothiazine-based new hole transporting materials for highly efficient green phosphorescent organic light-emitting diodes. *Molecules* **2018**, *23*, 713. [CrossRef] [PubMed]
4. Liu, F.; Zhang, Y.; Wang, H.; Zhang, S. Novel conjugated polymers prepared by direct (Hetero) arylation: An eco-friendly tool for organic electronics. *Molecules* **2018**, *23*, 408. [CrossRef] [PubMed]
5. Ali, B.; Khalid, M.; Asim, S.; Khan, M.U.; Iqbal, Z.; Hussain, A.; Hussain, R.; Ahmed, S.; Ali, A.; Hussain, A.; et al. Key electronic, linear and nonlinear optical properties of designed disubstituted quinoline with carbazole compounds. *Molecules* **2021**, *26*, 2760. [CrossRef]
6. Bracciale, M.P.; Kwon, G.; Ho, D.; Kim, C.; Santarelli, M.L.; Marrocchi, A. Synthesis, characterization, and thin-film transistor response of Benzoipentahelicene-3,6-dione. *Molecules* **2022**, *27*, 863. [CrossRef]
7. Guo, R.; Leng, P.; Zhang, Q.; Wang, Y.; Lv, X.; Sun, S.; Ye, S.; Duan, Y.; Wang, L. Donor engineering for diphenylsulfone derivatives with both thermally activated delayed fluorescence and aggregation-induced emission properties. *Dyes Pigm.* **2021**, *184*, 108781. [CrossRef]
8. Chen, G.; Qiu, Z.; Tan, J.-H.; Chen, W.-C.; Zhou, P.; Xing, L.; Ji, S.; Qin, Y.; Zhao, Z.; Huo, Y. Deep-blue organic light-emitting diodes based on push-pull π-extended imidazole-fluorene hybrids. *Dyes Pigm.* **2021**, *184*, 108754. [CrossRef]
9. Zheng, B.; Huo, L. Recent advances of dithienobenzodithiophene-based organic semiconductors for organic electronics. *Sci. China Chem.* **2021**, *64*, 358–384. [CrossRef]
10. Mokhtar, S.M.A.; Alvarez de Eulate, E.; Yamada, M.; Prow, T.W.; Evans, D.R. Conducting polymers in wearable devices. *Med. Devices Sens.* **2021**, *4*, e10160. [CrossRef]
11. Che, Y.; Zhang, Y.; Yang, Y.; Liu, C.-H.; Izquierdo, R.; Xiao, S.S.; Perepichka, D.F. Understanding the photovoltaic behavior of A-D-A molecular semiconductors through a permutation of end groups. *J. Org. Chem.* **2020**, *85*, 52–61. [CrossRef]
12. Zhao, M.; Yang, X.; Tsui, G.C.; Miao, Q. Trifluoromethylation of anthraquinones for n-Type organic semiconductors in field effect transistors. *J. Org. Chem.* **2020**, *85*, 44–51. [CrossRef] [PubMed]
13. Ghosh, S.; Shankar, S.; Philips, D.S.; Ajayaghosh, A. Diketopyrrolopyrrole-based functional supramolecular polymers: Next-generation materials for optoelectronic applications. *Mater. Today Chem.* **2020**, *16*, 100242. [CrossRef]
14. Arias-Gómez, A.; Godoy, A.; Portilla, J. Functional Pyrazolo1,5-apyrimidines: Current approaches in synthetic transformations and uses as an antitumor scaffold. *Molecules* **2021**, *26*, 2708. [CrossRef] [PubMed]
15. Ravichandiran, P.; Boguszewska-Czubara, A.; Masłyk, M.; Bella, A.P.; Johnson, P.M.; Subramaniyan, S.A.; Shim, K.S.; Yoo, D.J. A phenoxazine-based fluorescent chemosensor for dual channel detection of Cd^{2+} and CN-ions and its application to bio-imaging in live cells and zebrafish. *Dyes Pigm.* **2020**, *172*, 107828. [CrossRef]
16. Municoy, S.; Álvarez Echazú, M.I.; Antezana, P.E.; Galdopórpora, J.M.; Olivetti, C.; Mebert, A.M.; Foglia, M.L.; Tuttolomondo, M.V.; Alvarez, G.S.; Hardy, J.G.; et al. Stimuli-Responsive materials for tissue engineering and drug delivery. *Int. J. Mol. Sci.* **2020**, *21*, 4724. [CrossRef]
17. Shi, Y.; Zhang, F.; Linhardt, R.J. Porphyrin-based compounds and their applications in materials and medicine. *Dyes Pigm.* **2021**, *188*, 109136. [CrossRef]
18. Li, J.; Liu, Y.; Xu, Y.; Li, L.; Sun, Y.; Huang, W. Recent advances in the development of NIR-II organic emitters for biomedicine. *Coord. Chem. Rev.* **2020**, *415*, 213318. [CrossRef]

19. Wu, D.; Zhou, J.; Creyer, M.N.; Yim, W.; Chen, Z.; Messersmith, P.B.; Jokerst, J.V. Phenolic-enabled nanotechnology: Versatile particle engineering for biomedicine. *Chem. Soc. Rev.* **2021**, *50*, 4432–4483. [CrossRef]
20. Khan, S.A.; Kumar, P. Photophysical and Physicochemical investigation of newly synthesized polycyclic pyrazoline-benzothiazole as fluorescence Chemosensor for the detection of Cu^{2+} metal ion. *Polycycl. Aromat. Compd.* **2021**, *41*, 576–592. [CrossRef]
21. Tavallali, H.; Deilamy-Rad, G.; Parhami, A.; Asghari, K.; Ahmadi, A. Bismuth triggered selective colorimetric naked-eye detection for oxalate ions based on bromopyrogallol red that works as a molecular keypad lock. *Int. J. Environ. Anal. Chem.* **2021**, *101*, 648–667. [CrossRef]
22. Diana, R.; Caruso, U.; Di Costanzo, L.; Gentile, F.S.; Panunzi, B. Colorimetric recognition of multiple first-row transition metals: A single water-soluble chemosensor in acidic and basic conditions. *Dyes Pigm.* **2021**, *184*, 108832. [CrossRef]
23. Sánchez-Portillo, P.; Hernández-Sirio, A.; Godoy-Alcántar, C.; Lacroix, P.G.; Agarwal, V.; Santillán, R.; Barba, V. Colorimetric metal ion (II) Sensors Based on imine boronic esters functionalized with pyridine. *Dyes Pigm.* **2021**, *186*, 108991. [CrossRef]
24. Wang, S.; Zhu, B.; Wang, B.; Fan, P.; Jiu, Y.; Zhang, M.; Jiang, L.; Hou, J.-T. A highly selective phenothiazine-based fluorescent chemosensor for phosgene. *Dyes Pigm.* **2020**, *173*, 107933. [CrossRef]
25. Samanta, S.K.; Maiti, K.; Ali, S.S.; Guria, U.N.; Ghosh, A.; Datta, P.; Mahapatra, A.K. A solvent directed D-π-A fluorescent chemodosimeter for selective detection of hazardous hydrazine in real water sample and living cell. *Dyes Pigm.* **2020**, *173*, 107997. [CrossRef]
26. Malkondu, S.; Erdemir, S.; Karakurt, S. Red and blue emitting fluorescent probe for cyanide and hypochlorite ions: Biological sensing and environmental analysis. *Dyes Pigm.* **2020**, *174*, 108019. [CrossRef]
27. Bathula, C.; Henry, O.; Ashok Kumar, K.; Subalakshmi, K.; Jana, A.; Rabani, I.; Choi, J.-H.; Jeon, J.-H.; Kim, H.-S. Facile synthesis of an indacenodithiophene-based conjugated polymer for acid vapor sensing. *Dyes Pigm.* **2021**, *184*, 108847. [CrossRef]
28. Nagarajan, R.; Varadaraju, C.; Lee, K.H. Recent advancements in the role of N-heterocyclic receptors on heavy metal ion sensing. *Dyes Pigm.* **2021**, *191*, 109331. [CrossRef]
29. Rashdan, H.R.M.; Farag, M.M.; El-Gendey, M.S.; Mounier, M.M. Toward rational design of novel anti-cancer drugs based on targeting, solubility, and bioavailability exemplified by 1,3,4-thiadiazole derivatives synthesized under solvent-free conditions. *Molecules* **2019**, *24*, 2371. [CrossRef]
30. Liu, L.; Lei, Y.; Zhang, J.; Li, N.; Zhang, F.; Wang, H.; He, F. Rational design for multicolor flavone-based fluorophores with aggregation-induced emission enhancement characteristics and applications in mitochondria-imaging. *Molecules* **2018**, *23*, 2290. [CrossRef]
31. Cheng, H.-B.; Zhang, S.; Qi, J.; Liang, X.-J.; Yoon, J. Advances in application of azobenzene as a trigger in biomedicine: Molecular design and spontaneous assembly. *Adv. Mater.* **2021**, *33*, e2007290. [CrossRef]
32. Li, B.; Zhao, M.; Zhang, F. Rational design of Near-Infrared-II organic molecular dyes for bioimaging and biosensing. *ACS Mater. Lett.* **2020**, *2*, 905–917. [CrossRef]
33. Amabili, P.; Biavasco, F.; Brenciani, A.; Citterio, B.; Corbisiero, D.; Ferrazzano, L.; Fioriti, S.; Guerra, G.; Orena, M.; Rinaldi, S. Simple amphiphilic α-hydrazido acids: Rational design, synthesis, and in vitro bioactivity profile of a novel class of potential antimicrobial compounds. *Eur. J. Med. Chem.* **2020**, *189*, 112072. [CrossRef] [PubMed]
34. Jun, J.V.; Chenoweth, D.M.; Petersson, E.J. Rational design of small molecule fluorescent probes for biological applications. *Org. Biomol. Chem.* **2020**, *18*, 5747–5763. [CrossRef] [PubMed]
35. Ghosh, N.N.; Saha, S.; Pramanik, A.; Sarkar, P.; Pal, S. Molecular design of porphyrin dyes using different electron-withdrawing moieties for high performance dye-sensitized solar cells. *Comput. Theor. Chem.* **2020**, *1182*, 112846. [CrossRef]
36. Dai, J.; Wu, X.; Ding, S.; Lou, X.; Xia, F.; Wang, S.; Hong, Y. Aggregation-Induced emission photosensitizers: From molecular design to photodynamic therapy. *J. Med. Chem.* **2020**, *63*, 1996–2012. [CrossRef]
37. Bronstein, H.; Nielsen, C.B.; Schroeder, B.C.; McCulloch, I. The role of chemical design in the performance of organic semiconductors. *Nat. Rev. Chem.* **2020**, *4*, 66–77. [CrossRef]
38. Poriel, C.; Rault-Berthelot, J. Blue Single-Layer organic light-emitting diodes using fluorescent materials: A molecular design view point. *Adv. Funct. Mater.* **2020**, *30*, 1910040. [CrossRef]
39. Gerasimova, T.P.; Burganov, T.I.; Katsyuba, S.A.; Kalinin, A.A.; Islamova, L.N.; Fazleeva, G.M.; Ahmadeev, B.S.; Mustafina, A.R.; Monari, A.; Assfeld, X.; et al. Halochromic luminescent quinoxalinones as a basis for pH-sensing in organic and aqueous solutions. *Dyes Pigm.* **2021**, *186*, 108958. [CrossRef]
40. Kurishita, Y.; Kohira, T.; Ojida, A.; Hamachi, I. Rational design of FRET-based ratiometric chemosensors for in vitro and in cell fluorescence analyses of nucleoside polyphosphates. *J. Am. Chem. Soc.* **2010**, *132*, 13290–13299. [CrossRef]
41. Bamesberger, A.; Schwartz, C.; Song, Q.; Han, W.; Wang, Z.; Cao, H. Rational design of a rapid fluorescent approach for detection of inorganic fluoride in MeCN–H$_2$O: A new fluorescence switch based on N-aryl-1,8-naphthalimide. *New J. Chem.* **2014**, *38*, 884–888. [CrossRef]
42. Wang, B.; Han, J.; Zhang, H.; Bender, M.; Biella, A.; Seehafer, K.; Bunz, U.H.F. Detecting counterfeit brandies. *Chem. Eur. J.* **2018**, *24*, 17361–17366. [CrossRef] [PubMed]
43. Fu, Z.-H.; Qin, J.-C.; Wang, Y.-W.; Peng, Y.; Zhang, Y.-M.; Zhao, D.-M.; Zhang, Z.-H. A quinoline-based chromogenic and ratiometric fluorescent probe for selective detection of Mg^{2+} ion: Design, synthesis and its application in salt lake brines and bioimaging. *Dyes Pigm.* **2021**, *185*, 108896. [CrossRef]

44. Jia, Y.; Li, P.; Song, W.; Zhao, G.; Zheng, D.; Li, D.; Wang, Y.; Wang, J.; Li, C.; Han, K. Rational design of a profluorescent substrate for S-Adenosylhomocysteine hydrolase and its applications in bioimaging and inhibitor screening. *ACS Appl. Mater. Interfaces* **2016**, *8*, 25818. [CrossRef] [PubMed]

45. Zhai, B.; Hu, Z.; Peng, C.; Liu, B.; Li, W.; Gao, C. Rational design of a colorimetric and fluorescence turn-on chemosensor with benzothiazolium moiety for cyanide detection in aqueous solution. *Spectrochim. Acta A Mol. Biomol. Spectrosc.* **2020**, *224*, 117409. [CrossRef]

46. Han, Q.; Liu, X.; Wang, X.; Yin, R.; Jiang, H.; Ru, J.; Liu, W. Rational design of a lysosomal-targeted ratiometric two-photon fluorescent probe for imaging hydrogen polysulfides in live cells. *Dyes Pigm.* **2020**, *173*, 107877. [CrossRef]

47. Lu, Y.; Ruan, G.; Du, W.; Li, J.; Yang, N.; Wu, Q.; Lu, L.; Zhang, C.; Li, L. Recent progress in rational design of fluorescent probes for Fe2+ and bioapplication. *Dyes Pigm.* **2021**, *190*, 109337. [CrossRef]

48. Peng, Z.; Shi, L.; Zeng, X.; Yang, S.; Xiao, J.; Gong, S.; Xiang, H.; Shao, G. Rational design of the ratiometric fluorescent probes for sulfur dioxide derivatives and the study on the sensing performance of cyano-containing groups. *Dyes Pigm.* **2021**, *186*, 108972. [CrossRef]

49. Wang, B.; Anslyn, E.V. *Chemosensors: Principles, Strategies and Applications*; Wiley-Blackwell: Oxford, UK, 2011.

50. Chua, M.H.; Shah, K.W.; Zhou, H.; Xu, J. Recent advances in aggregation-induced emission chemosensors for anion sensing. *Molecules* **2019**, *24*, 2711. [CrossRef]

51. Li, Y.; Zhong, H.; Huang, Y.; Zhao, R. Recent advances in Aiegens for metal ion biosensing and bioimaging. *Molecules* **2019**, *24*, 4593. [CrossRef]

52. Kwon, N.; Hu, Y.; Yoon, J. Fluorescent Chemosensors for various analytes including reactive oxygen species, biothiol, metal ions, and toxic gases. *ACS Omega* **2018**, *3*, 13731–13751. [CrossRef]

53. Wu, D.; Sedgwick, A.C.; Gunnlaugsson, T.; Akkaya, E.U.; Yoon, J.; James, T.D. Fluorescent chemosensors: The past, present and future. *Chem. Soc. Rev.* **2017**, *46*, 7105–7123. [CrossRef] [PubMed]

54. Borelli, M.; Iasilli, G.; Minei, P.; Pucci, A. Fluorescent polystyrene films for the detection of volatile organic compounds using the twisted intramolecular charge transfer mechanism. *Molecules* **2017**, *22*, 1306. [CrossRef] [PubMed]

55. Alam, A.U.; Qin, Y.; Nambiar, S.; Yeow, J.T.; Howlader, M.M.; Hu, N.-X.; Deen, M.J. Polymers and organic materials-based pH sensors for healthcare applications. *Prog. Mater. Sci.* **2018**, *96*, 174–216. [CrossRef]

56. Bindhu, M.R.; Umadevi, M. Silver and gold nanoparticles for sensor and antibacterial applications. *Spectrochim. Acta A Mol. Biomol. Spectrosc.* **2014**, *128*, 37–45. [CrossRef]

57. Chah, S.; Hammond, M.R.; Zare, R.N. Gold nanoparticles as a colorimetric sensor for protein conformational changes. *Chem. Biol.* **2005**, *12*, 323–328. [CrossRef]

58. Horak, E.; Kassal, P.; Murković Steinberg, I. Benzimidazole as a structural unit in fluorescent chemical sensors: The hidden properties of a multifunctional heterocyclic scaffold. *Supramol. Chem.* **2018**, *30*, 838–857. [CrossRef]

59. Wang, T.; Zhang, N.; Bai, W.; Bao, Y. Fluorescent chemosensors based on conjugated polymers with N-heterocyclic moieties: Two decades of progress. *Polym. Chem.* **2020**, *11*, 3095–3114. [CrossRef]

60. Lakowicz, J.R. *Principles of Fluorescence Spectroscopy*; Springer: New York, NY, USA, 2006.

61. Schönhaber, J.; Frank, W.; Müller, T.J.J. Insertion-coupling-cycloisomerization domino synthesis and cation-induced halochromic fluorescence of 2,4-diarylpyrano[2,3-*b*]indoles. *Org. Lett.* **2010**, *12*, 4122–4125. [CrossRef]

62. Wilcke, T.; Glißmann, T.; Lerch, A.; Karg, M.; Müller, T.J.J. Acidochromic Turn-on 2,4-Diarylpyrano[2,3-*b*]indole Luminophores with Solubilizing Groups for A Broad Range of Polarity. *ChemistrySelect* **2018**, *3*, 10345–10351. [CrossRef]

63. Mitsumori, S.; Tsuri, T.; Honma, T.; Hiramatsu, Y.; Okada, T.; Hashizume, H.; Inagaki, M.; Arimura, A.; Yasui, K.; Asanuma, F.; et al. Synthesis and biological activity of various derivatives of a novel class of potent, selective, and orally active prostaglandin D2 receptor antagonists. 1. Bicyclo2.2.1heptane derivatives. *J. Med. Chem.* **2003**, *46*, 2436–2445. [CrossRef]

64. Chimenti, F.; Fioravanti, R.; Bolasco, A.; Chimenti, P.; Secci, D.; Rossi, F.; Yáñez, M.; Orallo, F.; Ortuso, F.; Alcaro, S. Chalcones: A valid scaffold for monoamine oxidases inhibitors. *J. Med. Chem.* **2009**, *52*, 2818–2824. [CrossRef] [PubMed]

65. Reichardt, C. Solvatochromic dyes as solvent polarity indicators. *Chem. Rev.* **1994**, *94*, 2319–2358. [CrossRef]

66. Bourguignon, L.Y.; Chu, A.; Jin, H.; Brandt, N.R. Ryanodine receptor-ankyrin interaction regulates internal Ca^{2+} release in mouse T-lymphoma cells. *J. Biol. Chem.* **1995**, *270*, 17917–17922. [CrossRef] [PubMed]

67. Altura, B.M.; Carella, A.; Altura, B.T. Adverse effects of tris, hepes and mops buffers on contractile responses of arterial and venous smooth muscle induced by prostaglandins. *Prostaglandins Med.* **1980**, *5*, 123–130. [CrossRef]

68. Provencher, S.W. A constrained regularization method for inverting data represented by linear algebraic or integral equations. *Comput. Phys. Commun.* **1982**, *27*, 213–227. [CrossRef]

69. Jones, G.; Jackson, W.R.; Choi, C.Y.; Bergmark, W.R. Solvent effects on emission yield and lifetime for coumarin laser dyes. Requirements for a rotatory decay mechanism. *J. Phys. Chem.* **1985**, *89*, 294–300. [CrossRef]

70. Moore, J.W.; Pearson, R.G.; Frost, A.A. *Kinetics and Mechanism*; Wiley: New York, NY, USA, 1981.

71. Shirahase, H.; Takahashi, K.; Shoji, Y. Novel Aromatic Compound and Use Thereof. Patent WO2015030189, 5 March 2015.

72. Pisula, W.; Kastler, M.; Wasserfallen, D.; Pakula, T.; Müllen, K. Exceptionally long-range self-assembly of hexa-peri-hexabenzocoronene with dove-tailed alkyl substituents. *J. Am. Chem. Soc.* **2004**, *126*, 8074–8075. [CrossRef]

73. Lauter, U.; Meyer, W.H.; Enkelmann, V.; Wegner, G. Supramolecular structures of poly(p-phenylenes) with oxyethylene side chains and their mixtures with lithium salts. *Macromol. Chem. Phys.* **1998**, *199*, 2129–2140. [CrossRef]

74. Li, Y.; Urbas, A.; Li, Q. Synthesis and characterization of light-driven dithienylcyclopentene switches with axial chirality. *J. Org. Chem.* **2011**, *76*, 7148–7156. [CrossRef]

75. Tsai, C.; Jamison, J.M.; Summers, J.L. Ascorbate, Vitamin K3, and Hydroxytolans in the Treatment of Cancer. Patent WO2008157745, 24 December 2008.